Heliyon 10 (2024) e28793

Contents lists available at ScienceDirect

Heliyon

journal homepage: www.cell.com/heliyon

Research article

Simple and sensitive sandwich-like electrochemical immunosensing strategy for D-dimer based on cyclodextrin-carbon nanotube and nanogold-ferrocene

Sheng Lin [1], Jing Wang [1], Xiaoqin Wang, Suqin Xia, Ling Wu [*]

Fujian Maternity and Child Health Hospital, College of Clinical Medicine for Obstetrics & Gynecology and Pediatrics, Fujian Medical University, Fuzhou, PR China

ARTICLE INFO

Keywords:
D-dimer
Electrochemical detection
Immunosensor
Sandwich-like
Cancer

ABSTRACT

D-dimer is a very important biomarker about sepsis, pulmonary thromboembolism and atherosclerosis, thus designing effective and sensitive method for its detection is of great significance. Herein, by synthesizing β-cyclodextrin-carbon nanotube nanohybrid (CNTs-CD) as the carrier to assemble the initial antibody (Ab_1) of D-dimer, immobilizing secondary antibody (Ab_2) and sulfydryl ferrocene (Fc) on the nanogold (Au) particles surface as the signaling amplifier (Ab_2-Au-Fc), a low cost, simple, sensitive and effective sandwich-like electrochemical immunosensing (SEI) platform of D-dimer was proposed in this work for the first time. Briefly, CNTs shows large specific area and superior electroconductivity, and CD provides high host guest recognition ability that could bound with Ab_1; meanwhile, the Fc probe offers stable current response which are proportionable positively to the level of D-dimer. Under the best conditions, the designed SEI platform exhibits prominent analytical performances for D-dimer: low detection limit of 3.0 ng mL^{-1} and large linearity of 10.0–800.0 ng mL^{-1}. In addition, the selectivity, stability and reproducibility as well as real applications of the proposed SEI assay were evaluated and the obtained results are satisfactory.

1. Introduction

As a soluble fibrin degradation product, D-dimer is a very important biomarker which presents elevated in the blood from the patients with sepsis, pulmonary thromboembolism and atherosclerosis [1–3]. Generally, the clinical criteria of D-dimer in the healthy individuals is 0.5 μg mL^{-1}, an increased concentration of D-dimer suggests the risk from myocardial infarction and is listed as an effective biomarker for pathological coagulation [4,5]. Presently, there are several analytical methodologies developed for D-dimer detection, such as enzyme-linked immunosorbent assays, chemiluminescence, latex agglutination and whole blood agglutination [6–9]. However, the performance characteristics of these methods are not very uniform, endowing it a challenge to standardize the sensing system and compare the results between different works, which restrained their clinical application [10–12]. Consequently, developing reproducible and accurate method for the effective detection of D-dimer is very necessary [13]. In this context, the electrochemical technology is considered as a superior alternative to the conventional analytical means for the clinical biomarkers

* Corresponding author.
E-mail address: 13599040300@139.com (L. Wu).
[1] These authors contributed equally to this work.

https://doi.org/10.1016/j.heliyon.2024.e28793
Received 10 January 2024; Received in revised form 25 March 2024; Accepted 25 March 2024
Available online 26 March 2024

providing the superiorities of being rapid, easy operation, inexpensive, robust and sensitive.

Indeed recently, there are several interesting electrochemical sensors developed for the detection of D-dimer, but designing novel electrochemical sensing method for D-dimer is still highly important [14–16]. As widely-utilized detection method, the sandwich-like electrochemical immunosensing (SEI) has attracted many attentions owing to its high sensitivity and signal amplification [17–20], while there is no SEI assay reported to detect D-dimer. Based on these advantages, this work was dedicated to develop a sensitive and effective SEI platform to detect of D-dimer. Generally, SEI mainly includes 2 key parts: one is the carrier that is utilized to immobilize the initial antibody (Ab_1), the other is the signal amplifier which is used to immobilize Ab_2 and generate the signal referred to the target concentration [21–23].

As is well-known, carbon nanotubes (CNTs) display many superiorities, e.g., low cost, high surface area and conductivity, endowing CNTs to be a desirable carrier to assemble Ab_1 for constructing SEI system of D-dimer, but the inherent van der Waals interaction makes CNTs easy to bundle together, inducing the poor solubility in water and severe restriction in real applications [24–26]. β-cyclodextrin (CD) is an interesting oligosaccharide, which is toroidal in shape and offers a hydrophilic exterior along with a hydrophobic cavity. This special structure not offers high host-guest recognition ability and enables CD molecules bind selectively with antibodies, but can enhance the solubility and dispersibility of CD-based nanomaterials [27–29]. These superiorities made us convinced CD may be a superior candidate to modify CNTs for developing SEI platform of D-dimer.

Another key element for SEI is to design the related signal amplifier. An universally accessible and available noble metal, nanogold (Au) nanoparticle, exhibits high conductivity and biocompatibility along with superior electrocatalytic property, and it also can be modified easily with –SH, $–NH_2$ and –COOH [30,31]. Furthermore, SH-ferrocene (Fc) is an used widely probe since it possesses high electroactivity and can assemble to the Au surface [32,33]. Based on these features, herein, Ab_2 and Fc were assembled on the Au surface to form Ab_2-Au-Fc and be used as signalling amplifier; meanwhile, CD modified CNTs nanocomposites (CNTs-CD) was synthesized as the carrier to assemble Ab_1 via host guest bond (CNTs offer high surface area and conductivity for immobilizing CD, while CD can bond Ab1 via host guest recognition), hence a novel SEI strategy was successfully designed in this work to detect D-dimer for the first time: In the presence of D-dimer, Ab_2-Au-Fc/D-dimer/Ab_1-CNTs-CD sandwich structure is generated and the current response of Fc is positively proportional to the D-dimer concentration, thus realizing highly sensitive detection for D-dimer (Scheme 1). This works provided a novel and effective method for the detection of D-dimer, it's expected that it offers great potential applications.

2. Experimental

2.1. Synthesization of CNTs-CD and Ab_2-Au-Fc

With the assistance of Py group, Py-CD could tightly stick to CNTs via π-πinteractions: briefly, 20.0 mg CNTs and 5.0 mg Py-CD was mixed in 40.0 mL DMF containing and stirred continuously for ~2 h. Next, the formed mixture was filtered, washed and dried. In order to assemble Ab_2-Au-Fc, the Au nanoparticles were firstly prepared. In brief, 0.1 mL sodium citrate (0.2 M) was added dropwise to 3.0 mL $HAuCl_4$ solution (0.2 mg mL^{-1}) and sequentially heated at 60 °C for ~2 h. Then, 10.0 μL Fc probe solution of 0.5 mM and 5.0 μL Ab_2 of 80.0 μg mL^{-1} and was added in to the obtained Au solution of 1.0 mL for generating signaling amplifier Ab_2-Au-Fc.

2.2. Fabrication of SEI assay for D-dimer

The polished GCE was coated with 9.0 μL CNTs-CD solution and dried via an infrared light. Next, 5.0 μL Ab_1 was incubated on the CNTs-CD/GCE surface and BSA was used to restrain the non-specific adsorption. Then, the formed Ab_1-CNTs-CD/GCE suffered the interaction with D-dimer and D-dimer/Ab_1-CNTs-CD/GCE was sequentially immersed in the Ab_2-Au-Fc solution to generate a SEI structure. To avoid the influence from the temperature, the related experiments were carried out at 25 ± 2 °C.

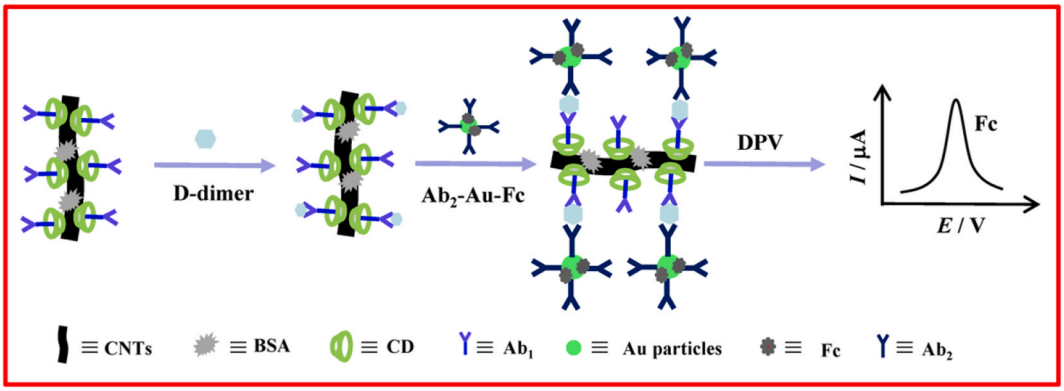

Scheme 1. Illustrations for fabricating the SEI assay of D-dimer.

3. Results and discussions

3.1. Characterizations of CNTs-CD and Au nanoparticles

TEM was introduced to study the morphologies of CNTs-CD. As exhibited in Fig. 1A, it shows clearly that CNTs exhibits tubular nanostructure with the diameter of 6.0 nm. And CD molecules were modified uniformly on CNTs surface with the thickness of ~0.5 nm (Fig. 1B and C). Then, the CNTs-CD dispersibility was studied in water (Figure S1). It was noted the dispersion ability of CNTs is considerable poor, but a dark and homogeneous dispersion was observed for the formed CNTs-CD owing to the hydrophilic external cavity of CD, suggesting the as-synthesized CNTs-CD hybrid has superior dispersibility, which is beneficial to efficiently restrain the CNTs aggregation and improve the sensing performance. Furthermore, TEM was used also to investigate the Au nanoparticles. From Fig. 2A, it was found the Au sizes are uniform, the average size (diameter) is about 5.0 nm (Fig. 2B).

Next, the prepared CNTs-CD was studied further by FT-IR spectroscopy and Raman spectroscopy (Fig. 3). From the FT-IR spectroscopy, the CNTs shows only C–C and C═C band at 1125 and 1575 cm^{-1}, respectively; while CNTs-CD shows typical β-CD features of 1028, 2922 and 3440 cm^{-1}, which refer respectively to C–O/C–C stretching/O–H bending vibrations, CH_2 and O–H stretching vibrations. As for the Raman spectroscopy (Fig. 3B), the peak at 1315 cm^{-1} was assigned to the A_{1g} breathing mode of disorder structure graphite about the D band, and the peak of 1562 cm^{-1} can be assigned to the E_{2g} structure mode about the G band. The intensity ratio of the D and G band (denoted as I_D/I_G) can be utilized to reveal the functionalization degree of carbon material. The obtained results revealed the value of the I_D/I_G ratio of CNTs is 0.08, whereas the I_D/I_G ratio (0.063) of the CNTs-CD is smaller than that of CNTs, indicating that the CD immobilization has un-detrimental effect on the CNTs structure.

Finally, the prepared CNTs-CD hybrid was investigated also by thermogravimetric analysis (TGA) and the related results were displayed in Figure S2. For the pristine CNTs, there is almost no weight loss in the measured temperature range (curve a). However, for CNTs-CD, an important weight loss (~28.5 wt%) was observed from ~250 °C to 800 °C owing to the CD decomposition, suggesting there are abundant CD molecules immobilized on the surface of CNTs.

3.2. Construction of SEI platform of D-dimer

The feasibility of the proposed SEI for D-dimer was investigated by differential pulse voltammetry (DPV) technology. Fig. 4 showed the DPV curves of Ab_1-CNTs-CD/GCE before and after its interaction with D-dimer and sequentially incubated in Ab_2-Au-Fc solution. The results demonstrated there is nearly no DPV peak current appeared in the absence of D-dimer. Interestingly, a very strong oxidation current of Fc was found at ~0.25 V in the presence of D-dimer. The reason is the antigen-Ab specific recognition between D-dimer and Ab could result the capture of Ab_2-Au-Fc to D-dimer/Ab_1-CNTs-CD, thus forming SEI structure (Ab_2-Au-Fc/D-dimer/Ab_1-CNTs-CD). These indicated the designed SEI proposal for D-dimer is feasible.

In order to know the best analytical performances for sensing D-dimer, several critical parameters were next optimized. Firstly, the amount of CNTs-CD dropped on the GCE surface was studied and the results were shown in Fig. 5A. As can be seen, the DPV current of Ab_2-Au-Fc/D-dimer/Ab_1-CNTs-CD/GCE increase with increase of the related amount from 3.0 to 9.0 μL. When the amount exceeds 9.0 μL, there is little change for the response current, thus 9.0 μL CNTs-CD dispersion was used. Fig. 5B showed the effect of the pH values of solution, it was noted that the current responses increase along with the increase of pH value from 4.5, reaching a maximum value at 7.0. The reason is that the overacidic or hyperalkaline conditions may pose some damage to the structures of antibodies and proteins. Fig. 5C and D displayed the influence from the interaction time of D-dimer and Ab, the obtained results indicated the best time for D-dimer and Ab_1 is 30 min (Fig. 5C), whereas that is 20 min for D-dimer and Ab_2 (Fig. 5D). Upon the above optimized conditions, the analytical ability of the constructed SEI for D-dimer was further evaluated. As displayed in Fig. 6A, the DPV current gradually strengthened with the D-dimer level increased from 10.0 ng mL^{-1} to 800.0 ng mL^{-1}. The corresponding regression equation is $I_p(\mu A) = 0.3433 + 0.0056C$ (ng mL^{-1}) ($R^2 = 0.992$) (Fig. 6B), and the achieved detection limit (LOD) is low to 3.0 ng mL^{-1} (S/N = 3) that is far lower than the clinical criteria, indicating the designed SEI assay can satisfy the demand in clinical diagnosis.

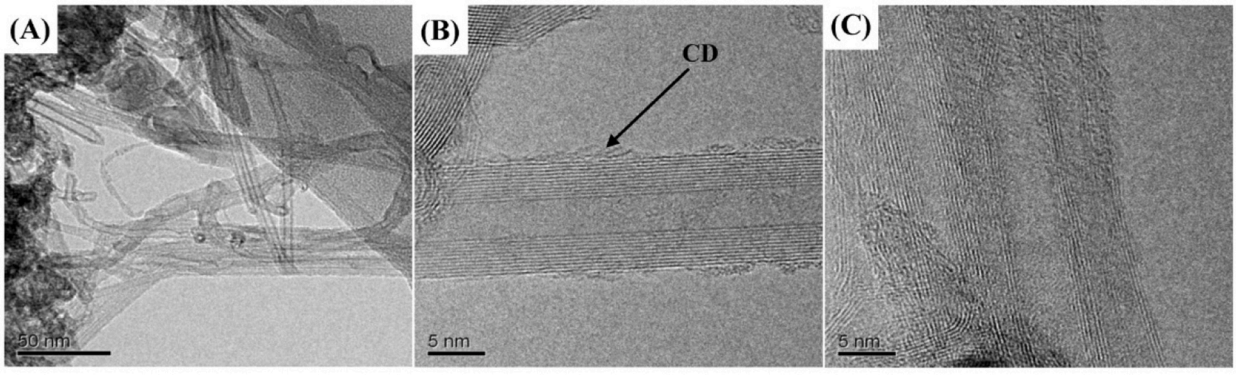

Fig. 1. TEM images of (A) CNTs and (B,C) CNTs-CD at different areas.

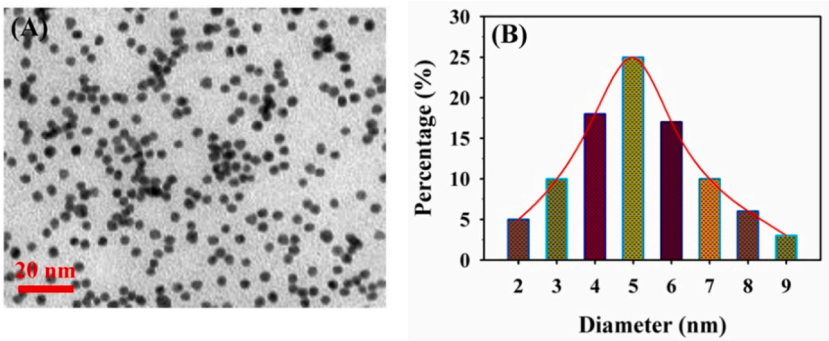

Fig. 2. TEM image (A) and size distribution (B) of Au nanoparticles.

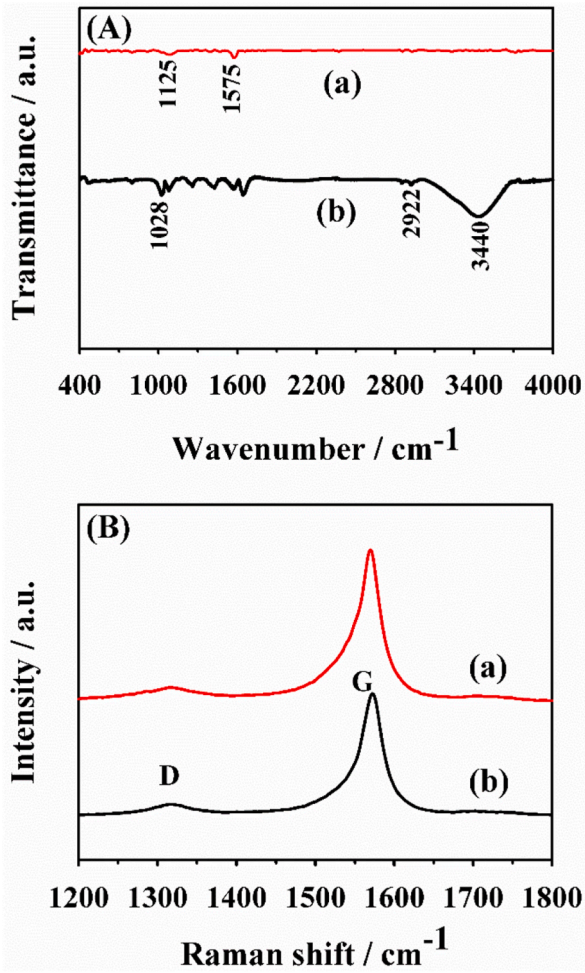

Fig. 3. (A) FT-IR and (B) Raman spectras of (a) CNTs and (b) CNTs-CD.

The selectivity from the designed SEI was investigated in the presence of several potential interfering substances. As displayed in Fig. 7, it was found there is nearly no change for the DPV current of Fc probe towards various potential interferes (10.0 times of D-dimer level). Then, the sensor stability was evaluated also (Figure S3A), and the results displayed the signalling response of SEI still remains nearly unchanged for four weeks via storing the sensing platforms at 4 °C. Next, the immunosensor reproducibility was studied via testing the current signalling of Fc probe at 8 independently-fabricated Ab_2-Au-Fc/D-dimer/Ab_1-CNTs-CD/GCE. As shown in Figure S3B, the RSD value for these sensing platforms is 2.7%. These obtained results demonstrated that the proposed SEI platform offers desirable selectivity and stability as well as reproducibility.

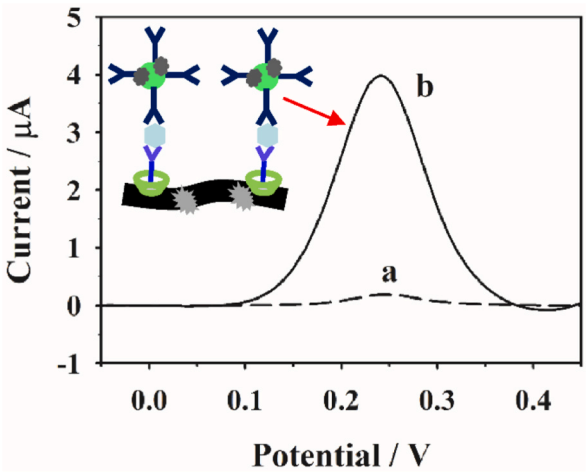

Fig. 4. DPV response of Ab_1-CNTs-CD/GCE before (a) and after (b) its interaction with D-dimer and sequentially incubated in Ab_2-Au-Fc solution.

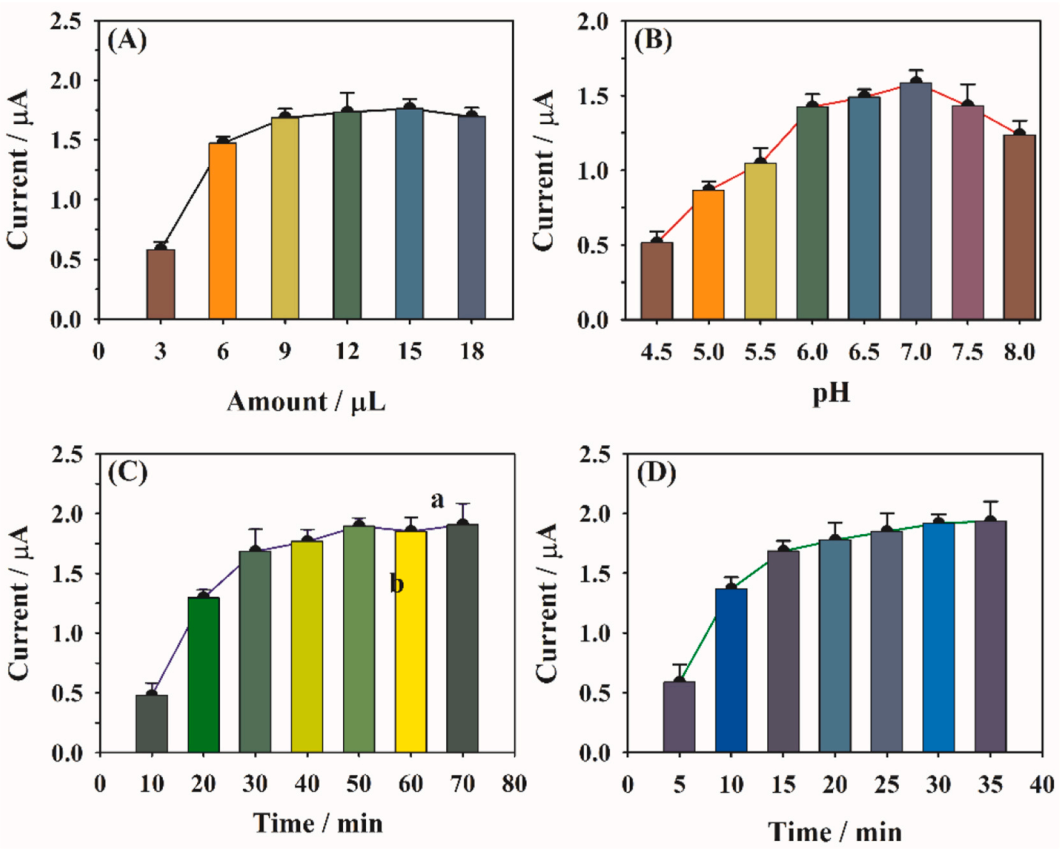

Fig. 5. The effects of (A) amount of CNTs-CD, (B) pH values of PBS, (C) interaction time of (a) Ab_1 with D-dimer and (b) D-dimer with Ab_2.

The real application of the designed proposal was evaluated by selecting standard addition method in the real human serum and compared with a standard method (HPLC). Different D-dimer levels were dropped in turn to the obtained samples, and sequentially the electrochemical response of the designed sensor towards these samples were tested, and the recovery was applied to express the sensor capability in real samples (Table S1). From the table, it was found the generated recoveries are 96.8%–98.2%, indicating the designed SEI platform provides satisfactory real applications capability for D-dimer detection.

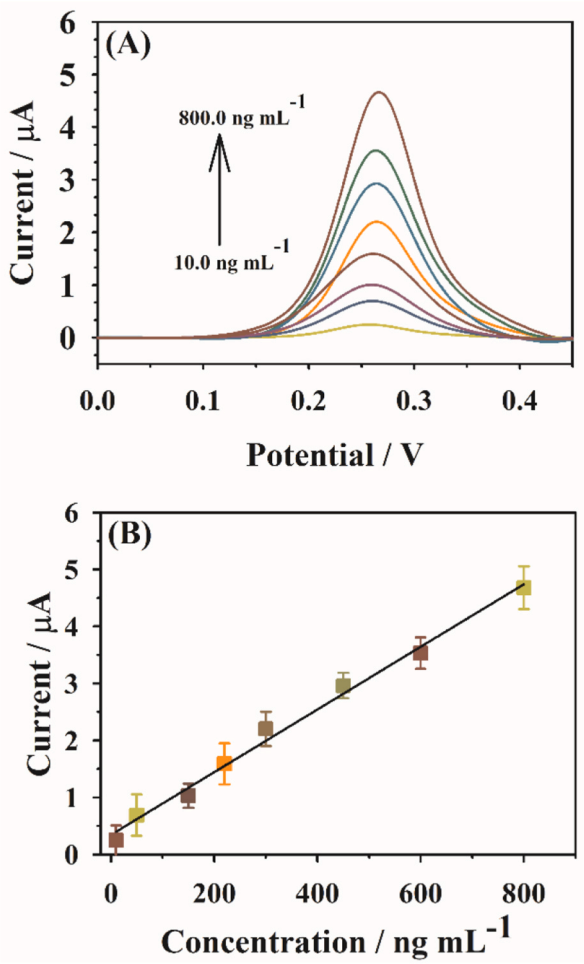

Fig. 6. (A) DPV responses of the design SEI assay at different concentrations of D-dimer (10.0–800.0 ng mL^{-1}); (B) the related calibration plot for D-dimer detection.

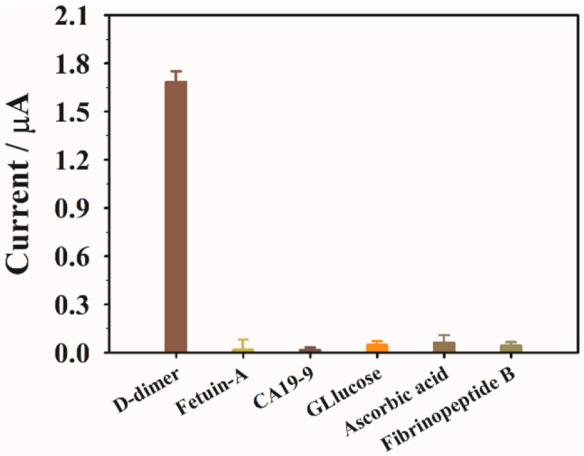

Fig. 7. Selectivity of the designed SEI platform for the detection of D-dimer.

4. Conclusion

In summary, a simple, low-cost and sensitive SEI platform was designed herein for the first time to detect D-dimer by preparing CNTs-CD nanohybrid as carrier to immobilize Ab_1 and Ab_2-Au-Fc as the signaling amplifier. Resulted from the specific antigen-antibody recognition reaction, a typical sandwich-like structure (Ab_2-Au-Fc/D-dimer/Ab_1-CNTs-CD) can be formed in the presence of D-dimer, and thus a related oxidation current from Fc probe can be observed. Through optimizing the various key parameters, the as-designed SEI platform exhibits superior analytical capabilities: wide linearity and low LOD; meanwhile, this sensor shows desirable selectivity, stability and reproducibility as well as real applications. However, the limitation of this sensor is the relative long detection time similar to the conventional SEM assay. Anyway, it's expected that the proposed SEI method for D-dimer detection has great potential applications in clinical application.

Data availability

Data will be made available on request.

CRediT authorship contribution statement

Sheng Lin: Writing – original draft, Methodology, Data curation, Conceptualization. **Jing Wang:** Validation, Software, Formal analysis. **Xiaoqin Wang:** Writing – review & editing, Resources, Investigation. **Suqin Xia:** Writing – review & editing, Validation, Software. **Ling Wu:** Writing – review & editing, Visualization, Supervision, Investigation, Funding acquisition.

Declaration of competing interest

The authors declare that they have no known competing financial interests or personal relationships that could have appeared to influence the work reported in this paper.

Acknowledgment

The work was financially supported by the Joint Funds for the innovation of science and Technology, Fujian province (2021Y9161).

Appendix A. Supplementary data

Supplementary data to this article can be found online at https://doi.org/10.1016/j.heliyon.2024.e28793.

References

[1] N. Tasić, T.R. Paixão, L.M. Gonçalves, Biosensing of D-dimer, making the transition from the central hospital laboratory to bedside determination, Talanta 207 (2020) 120270.
[2] S. Kotru, M. Klimuntowski, H. Ridha, Z. Uddin, A.A. Askhar, G. Singh, M.M. Howlader, Electrochemical sensing: a prognostic tool in the fight against COVID-19, TrAC, Trends Anal. Chem. 136 (2021) 116198.
[3] I. Ojeda, B. Garcinuño, M. Moreno-Guzmán, A. González-Cortés, M. Yudasaka, S. Iijima, F. Langa, P. Yáñez-Sedeño, J.M. Pingarrón, Carbon Nanohorns as a scaffold for the construction of disposable electrochemical immunosensing platforms. Application to the determination of fibrinogen in human plasma and urine, Anal. Chem. 86 (2014) 7749–7756.
[4] A.L.Y. Yokomichi, V. da Cruz Rodrigues, A. Moroz, M. Bertanha, S.J. Ribeiro, E. Deffune, M.L. Moraes, Detection of factor VIII and D-dimer biomarkers for venous thromboembolism diagnosis using electrochemistry immunosensor, Talanta 219 (2020) 121241.
[5] V.C. Rodrigues, M.L. Moraes, J.C. Soares, A.C. Soares, R. Sanfelice, E. Deffune, O.N. Oliveira Jr., Immunosensors made with layer-by-layer films on chitosan/gold nanoparticle matrices to detect D-dimer as biomarker for venous thromboembolism, Bull. Chem. Soc. Jpn. 91 (2018) 891–896.
[6] S. Li, Y. Jiang, S. Eda, J.J. Wu, Low-cost and desktop-fabricated biosensor for rapid and sensitive detection of circulating D-dimer biomarker, IEEE Sensor. J. 19 (2018) 1245–1251.
[7] Y. Wei, Y. Wang, J. Wang, X. Yang, H. Qi, Q. Gao, C. Zhang, Homogeneous electrogenerated chemiluminescence immunoassay for the detection of biomarkers by magnetic preconcentration on a magnetic electrode, Anal. Bioanal. Chem. 411 (2019) 4203–4211.
[8] C.F. Pereira, M.G.F. Sales, M.F. Frasco, A molecularly imprinted photonic polymer based on an inverse opal structure for sensing D-dimer at the point-of-care, Talanta 243 (2022) 123387.
[9] L.M. Schmidt-Speicher, K. Länge, Microfluidic integration for electrochemical biosensor applications, Curr. Opin. Electrochem. 29 (2021) 100755.
[10] S.M. Marques, A. Santos, L.M. Gonçalves, J.C. Sousa, P.R. Bueno, Sensitive label-free electron chemical capacitive signal transduction for D-dimer electroanalysis, Electrochim. Acta 182 (2015) 946–952.
[11] Z. Ibupoto, N. Jamal, K. Khun, X. Liu, M. Willander, A potentiometric immunosensor based on silver nanoparticles decorated ZnO nanotubes, for the selective detection of d-dimer, Sensor. Actuator. B Chem. 182 (2013) 104–111.
[12] S. Chebil, N. Macauley, T. Hianik, H. Korri-Youssoufi, Multiwalled carbon nanotubes modified by NTA-copper complex for label-free electrochemical immunosensor detection, Electroanalysis 25 (2013) 636–643.
[13] Q. Zeng, X. Dong, X. Ren, D. Wu, H. Ma, Y. Li, Q. Wei, Signal-enhanced immunosensor-based MOF-derived ZrO2 nanomaterials as electrochemiluminescence emitter for D-dimer detection, Anal. Chem. 95 (2023) 13596–13604.
[14] N. Tasić, L. Cavalcante, E. Deffune, M.S. Góes, T.R. Paixão, L.M. Gonçalves, Probeless and label-free impedimetric biosensing of D-dimer using gold nanoparticles conjugated with dihexadecylphosphate on screen-printed carbon electrodes, Electrochim. Acta 397 (2021) 139244.

[15] A. Lakey, Z. Ali, S.M. Scott, S. Chebil, H. Korri-Youssoufi, S. Hunor, A. Ohlander, M. Kuphal, J.S. Marti, Impedimetric array in polymer microfluidic cartridge for low cost point-of-care diagnostics, Biosens. Bioelectron. 129 (2019) 147–154.
[16] L. Fan, Y. Yan, B. Guo, M. Zhao, J. Li, X. Bian, H. Wu, W. Cheng, S. Ding, Trimetallic hybrid nanodendrites and magnetic nanocomposites-based electrochemical immunosensor for ultrasensitive detection of serum human epididymis protein 4, Sensor. Actuator. B Chem. 296 (2019) 126697.
[17] R. Ren, D. Lu, T. Liu, Development of a sandwich-type rat small intestine tissue sensor for detecting resveratrol and its receptors, Biomed. Microdevices 23 (2021) 13.
[18] P. Hashemi, A. Afkhami, B. Baradaran, R. Halabian, T. Madrakian, F. Arduini, T.A. Nguyen, H. Bagheri, Well-orientation strategy for direct immobilization of antibodies: development of the immunosensor using the boronic acid-modified magnetic graphene nanoribbons for ultrasensitive detection of lymphoma cancer cells, Anal. Chem. 92 (2020) 11405–11412.
[19] S. Parvin, P. Hashemi, A. Afkhami, M. Ghanei, H. Bagheri, Simultaneous determination of BoNT/A and/E using an electrochemical sandwich immunoassay based on the nanomagnetic immunosensing platform, Chemosphere 298 (2022) 134358.
[20] F. Fazlali, P. Hashemi, S.M. Khoshfetrat, R. Halabian, B. Baradaran, M. Johari-Ahar, P. Karami, A. Hajian, H. Bagheri, Electrochemiluminescent biosensor for ultrasensitive detection of lymphoma at the early stage using CD20 markers as B cell-specific antigens, Bioelectrochemistry 138 (2021) 107730.
[21] H. Xiao, S. Wei, M. Gu, Z. Chen, L. Cao, A sandwich-type electrochemical immunosensor using rGO-TEPA-Thi-Au as sensitive platform and CMK-3@ AuPtNPs as signal probe for AFP detection, Microchem. J. 170 (2021) 106641.
[22] M. Hervás, M.A. López, A. Escarpa, Electrochemical immunosensing on board microfluidic chip platforms, TrAC, Trends Anal. Chem. 31 (2012) 109–128.
[23] X. Jiang, W. Ding, Z. Lv, C. Rao, Highly sensitive electrochemical immunosensing for Listeria monocytogenes based on 3, 4, 9, 10-Perylene tetracarboxylic acid/graphene ribbons as a sensing platform and ferrocene/gold nanoparticles as an amplifier, Anal. Sci. 37 (2021) 1701–1706.
[24] A.U. Alam, M.J. Deen, Bisphenol A electrochemical sensor using graphene oxide and β-cyclodextrin-functionalized multi-walled carbon nanotubes, Anal. Chem. 92 (2020) 5532–5539.
[25] N. Hareesha, J.G. Manjunatha, A.M. Tighezza, M.D. Albaqami, M. Sillanpää, Electrochemical detection and quantification of catechol based on a simple and sensitive poly(riboflavin) modified carbon nanotube paste electrode, Heliyon 9 (2023).
[26] S.M. Khoshfetrat, P. Hashemi, A. Afkhami, A. Hajian, H. Bagheri, Cascade electrochemiluminescence-based integrated graphitic carbon nitride-encapsulated metal-organic framework nanozyme for prostate-specific antigen biosensing, Sensor. Actuator. B Chem. 348 (2021) 130658.
[27] X. Tu, F. Gao, X. Ma, J. Zou, Y. Yu, M. Li, F. Qu, X. Huang, L. Lu, Mxene/carbon nanohorn/β-cyclodextrin-Metal-organic frameworks as high-performance electrochemical sensing platform for sensitive detection of carbendazim pesticide, J. Hazard Mater. 396 (2020) 122776.
[28] B. Mirzaei, A. Zarrabi, A. Noorbakhsh, A. Amini, P. Makvandi, A reduced graphene oxide-β-cyclodextrin nanocomposite-based electrode for electrochemical detection of curcumin, RSC Adv. 11 (2021) 7862–7872.
[29] V.T. Veetil, A.D. Rajeeve, S. G.P, K.S. Manish Kumar, M. Bhagiyalakshmi, M. Vinoba, R. Yamuna, β-Cyclodextrin capped ZnS nanoparticles for CER-assisted colorimetric and spectrophotometric detection of Pb^{2+}, Cu^{2+}, and Hg^{2+} in an aqueous solution, Heliyon 9 (2023) e21850.
[30] W. Zhao, M. Wu, L. Mei, H. Li, Ultra-sensitive electrochemical determination of carcinoembryonic antigen by a sandwich immunosensor graphene oxide (GO)-Gold substrate and a silver-coated bovine serum albumin (BSA)-Platinum nanocomposite on a glassy carbon electrode (GCE), Anal. Lett. 55 (2022) 980–989.
[31] S. Han, W. Liu, M. Zheng, R. Wang, Label-free and ultrasensitive electrochemical DNA biosensor based on urchinlike carbon nanotube-gold nanoparticle nanoclusters, Anal. Chem. 92 (2020) 4780–4787.
[32] B. Wu, S. Yeasmin, Y. Liu, L.-J. Cheng, Sensitive and selective electrochemical sensor for serotonin detection based on ferrocene-gold nanoparticles decorated multiwall carbon nanotubes, Sensor. Actuator. B Chem. 354 (2022) 131216.
[33] X. Jiang, W. Ding, Z. Lv, C. Rao, Highly sensitive electrochemical immunosensing for Listeria monocytogenes based on 3,4,9,10-perylene tetracarboxylic acid/graphene ribbons as a sensing platform and ferrocene/gold nanoparticles as an amplifier, Anal. Sci. 37 (2021) 1701–1706.